

Flood Spatial Analysis Using LiDAR DEM

Study Area (Azozab locality - Khartoum state - Sudan)

Fatima Ibrahim^[1], Dieter Fritsch^[2]

^[1]Sudan University of Sciences and Technology, ^[2]Germany Stuttgart University

ABSTRACT

Flood is the deadliest type of severe weather. A flood is an overflow of water that submerges land that is usually dry. Floods can come on quickly or build gradually. It is a well-known fact that the integration/use of Geographic Information Systems (GIS) and remote sensing in Water Management is very helpful. This research was conducted in “Azozab” locality, Khartoum state, Sudan. The study area is bounded by longitudes 32°28'30" E - 32°28'45"E and latitudes 15°29'45" N - 15°31'45" N. The total study area “Azozab” is about 4.25 Km². Azozab used to be exposed to severe floods frequently and the last incident of flood was in August 2021. The materials used for this research were Light Detection And Ranging (LiDAR DEM 1), aerial photograph 2018 with spatial resolution of 0.3 m, a polylines shapefile containing flood extent lines in 1946, 1989, an existing protection bank, and field-collected GPS point coordinates. These materials were processed using ArcGIS 10.2, Archedro and QGIS3.4.3 to produce a 3-meters vertical interval contour map, 3D coordinates (X, Y, Z) of each of the flood extent lines 1946, 1989, and the existing protection bank, in addition to the drainage system of the study area. The point coordinates of the mentioned lines were plotted as graphs. It was found that the flood line 1946 was 4.59 km long, flood line 1989 was 4.57 km long, and the protection bank was 3.5 km long, therefore, the protection bank should be extended so that its length becomes equal to the length of 1946 flood line, i.e. to be extended by 1.09 Km. Furthermore, the elevations of the protection bank were found lower than the elevations of the higher flood line (1946 AD) for a distance of 3.060 km. This distance represents the length of the protection bank that requires increasing its elevations (i.e. constructing a higher embankment). It was found that the average height increment of the protection bank embankment wall equals 1.37 m approx. and protection wall thickness should be 0.5 m. Hence, the necessary building quantity equals 2,383.8 m³. It was found that (11) services such as mosques, education, health and other services are located inside the flood extent line of 1946, thus they were affected by flood. Also, (8) educational services were threatened by flood, because they are located in the vicinity of (i.e. located within 200 meters away from) the 1946 flood extent line.

Keywords:- Azozab locality, protection bank, Khartoum state.

I. INTRODUCTION

1-1 Overview:

Believe it or not, flooding is the deadliest type of severe weather. There's probably a lot about floods and flooding you don't know, such as what causes flooding?" and "Where does flooding occur?. A **flood** is an overflow of water that submerges land that is usually dry. Floods are an area of study in the discipline of hydrology. They are the most common and widespread natural severe weather events. Floods can come on quickly or build gradually.

Most floods are caused by one of the following activities: 1) Heavy rainfall, 2) Overflowing rivers, 3) Broken dams 4) Storm surge and tsunamis 5) Channels with steep banks 6) Lack of vegetation, and 7) Melting snow and ice.

Floods can have devastating effects on communities. Besides physical danger, floods also cause economic and social problems. The severest effect of flooding is death. It only takes six inches of water to wash a person away. Floods can also lead to death of people by destroying buildings and creating unsafe environments. One often-overlooked deadly effect of flooding comes from waterborne illnesses.

Since it only takes two feet of flood water to wash a car away, flooding can also cause great loss of property. Surely you've seen images of cars being washed away in flood waters. This is why it is so important to avoid flooded areas when driving. You don't want to be in your car when it gets washed away in the flood!, fig. (1).



Figure (1): Loss of Properties

Flooding also causes property damage to buildings by blowing out windows, sweeping away doors, corroding walls and foundations, and sending debris into infrastructure at a fast pace. Not to mention the furniture and items inside a house or business those are damaged when flood water makes its way inside, figure (2).



Figure (2): Collapse of buildings even if made of strong building materials

The economic impact of flooding can be devastating to a community. This comes from damage and disruption to things like communication towers, power plants, roads, bridges, and vegetation. This brings business activities in an area to a standstill.

Flooding hinders economic growth and development because of the high cost of relief and recovery associated with floods. In frequently flooded areas, there is less likely to be any investment in infrastructure and other developed activities.

Flooding can also create lasting trauma for victims. The loss of loved ones or homes can take a steep emotional toll, especially on children. Displacement from one's home and loss of livelihood can cause continuing stress and produce lasting psychological impacts.

In Sudan, on August, 20, 2020 Gr., based on the state-wise total of affected population, the highest number of affected population was recorded in Gezira state which was 27,780 persons, followed by Kassala which was 27,225 persons.

In this paper, the Inverse Distance Weighted (IDW) method was used as the basic spatial analysis (namely, interpolation) method to calculate the elevations of points along the 1946 flood extent line, 1989 flood extent line, and the existing protection bank. The calculation of the elevations of these points depends on the data points of the LiDAR DEM of the study area.

Spatial analysis is a kind of geographical analysis which involves statistical and manipulation techniques, which could be attributed to a specific geographic database (Cucala et al., 2018; Burrough, 2001).

The basic IDW interpolation formula is given in equation (1). Where x^* is an unknown value at a location (P), w_i is the weight, and x_i is a known point value, d_i is the distances of the known points from point P; n is the number of the known points used in the interpolation procedure for estimating the elevation of point P. The weight is inverse distance of the point (P) to each known point value (w_i) that is used in the calculation. Simply the weight can be calculated using equation (2).

$$x^* = \frac{w_1 x_1 + w_2 x_2 + w_3 x_3 + \dots + w_n x_n}{w_1 + w_2 + w_3 + \dots + w_n} \quad \text{Eq. (1)}$$

$$w_i = \frac{1}{d_{ix}^p} \quad \text{-----Equation (2)}$$

The assumption that makes interpolation a viable option is that spatially distributed objects are spatially correlated; in other words, things that are close together tend to have similar characteristics. For instance, if it is raining on one side of the street, you can predict with a high level of confidence that it is raining on the other side of the street. You would be less certain if it was raining across town and less confident still about the state of the weather in the next county.

1-1- The Study Area:

The study area is Azozab in Khartoum state, located between longitudes 32°28'30" - 32°28'45"E and latitudes 15°29'45" - 15°31'45" N as shown in figure (3). The total area is 4,247,568 m² and the Vegetated area is 665,328 m² (about 166

acre). Azozab is bounded at the north by Alazhari, at the east by Railway, at the west by the White Nile, and at the south by Aldabasin.

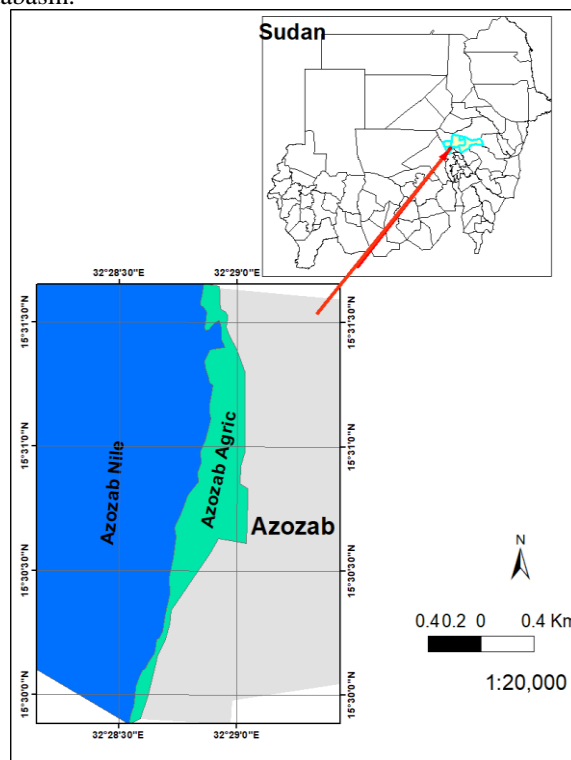


Figure (3): location map of the study area

1-2- Research Problem Statement:

The White Nile disastrous floods occur frequently in the study area (Azozab), in autumn, leading to many devastating and serious impacts on the community, such as loss of lives, property damage, economic effects, psychosocial effects, .. etc.

1-3- Research Question:

How can GIS techniques and remotely sensed data be used to investigate the effectiveness and design of a protection bank to mitigate or prevent the flood water impact in Azozab area?

1-4- Research Objectives:

- (1) To study the floods in the study area (Azozab) utilizing the space technologies (remotely sensed data such as LiDAR DEM1) and geographical information systems' capabilities for mapping and analyzing flood extent.
- (2) To produce topographic, surface water drainage systems and public administrative units (PAUs) maps etc. to obtain a clear picture of the flood extent in the study area, and to demarcate the services – in the study area which are affected by the flood, so that the right decision for avoiding or minimizing the adverse flood impacts can be taken.
- (3) To propose a method for enhancing the effectiveness and functionality of the existing flood protection bank in the study area.

Geostatistics is a collection of methods that allow you to estimate values for locations where no samples have been taken and also to assess the uncertainty of these estimates. These functions are critical in many decision-making

processes, as it is impossible in practice to take samples at every location in an area of interest, such as when the (x, y, z) coordinates of points are required to be calculated a long a flood extent line or a flood protection line,.

Many interpolation methods exist. Some are quite flexible and can accommodate different aspects of the sample data.

Geostatistics is a class of statistics used to analyze and predict the values associated with spatial or spatiotemporal phenomena. ArcGIS Geostatistical Analyst provides a set of tools that allow models that use spatial (and temporal) coordinates to be constructed. These models can be applied to a wide variety of scenarios and are typically used to generate predictions for unsampled locations, as well as measures of uncertainty for those predictions.

The first step, as in almost any data-driven study, is to closely examine the data. This typically starts by mapping the dataset, using a classification and color scheme that allow clear visualization of important characteristics that the dataset might present.

The second stage is to build the geostatistical model. This process can require several steps, depending on the objectives of the study (that is, the type(s) of information the model is supposed to provide) and the features of the dataset that have been deemed important enough to incorporate. At this stage, information collected during a rigorous exploration of the dataset and prior knowledge of the phenomenon determine how complex the model is and how good the interpolated values and measures of uncertainty will be.

(Geomatics, 2019) Many definitions have been formulated with regard to the concept of interpolation (e.g. Burrough 1986; McCullagh 1988; Robinson 1994). According to Burrough (1986): interpolation is the procedure of estimating the value of properties at unsampled sites within the area covered by existing point observations / data.

The Inverse Distance Weighted (IDW) method is widely recognized as the basic method in most systems that create and manage DEMs (Burrough 1986; Schut 1976). The main characteristic of this method is that all the points on the earth's surface are considered to be interdependent, on the basis of distance. Therefore, the calculation of altitudes in an area depends on the altitudes of the data points in the vicinity. According to (Wedajo, J., 2017) flood modeling, which is fully dependent on accurate and high-resolution DEM data, solves some of the limitations of Earth observation. As such, LiDAR system improved the performance of flood modeling via providing fine resolution DEM. The opportunities that LiDAR technology provided for flood mapping includes provision of accurate and high-resolution DEM data, relatively cost and time effective data collection system, capability of penetrating dense vegetation, improved flood model accuracy and fine scale flood modeling, adequate representation of man-made and topographic features, and capability of determining flood depth.

(SRCS report, July, 2008) revealed that in Khartoum state alone a number of 15,003 houses were damaged, of which 6,500 were partially damaged and 8,503 were completely damaged (cited by Altayeb H. Yahya, 2014). This was due to the unusual heavy rain witnessed by Khartoum state that caused a rush of storm water floods upon Umdawwanban

town and some villages within its vicinity. Since this town is already vulnerable because it has been built on a low land compared to its surroundings, it could not withstand the rushing floods and about 830 houses were completely destroyed while about 500 houses were partially destroyed. A similar disaster was encountered in Sharq Elneel Locality (Marabeea Elshareef and other neighboring towns) in the year 2013.

The suitability model built by the author was used to demarcate the suitable route for excavating a canal to divert some of the flood water away from Umdawwanban town and towards the Blue Nile.

2-Materials, tools, and Methods:

2-1- Materials:

The following materials were used for conducting this research:

1. Light Detection and Ranging Digital Elevation Model (LiDAR DEM 1), (Source: Surveying Department of Khartoum Locality).
2. An aerial photograph of the study area "Azozab" in the year 2018 (source: Surveying Department of Khartoum Locality),
3. Polylines shapefile showing flood extent in 1946, 1989, & the existing protection bank (source: Surveying Department - Khartoum Locality),
4. A polygons shapefile showing the public administration units (PAUs) of Azozab "source: Surveying Department - Khartoum Locality" but later digitized by the authors from image 2018).
5. A table containing the population of the PAUs, obtained from Jabal Awliya locality.
6. Point coordinates obtained by the authors through field work carried out using the Global Positioning System (GPS) navigator on (Sept., 2, 2021).

2-2- Tools:

- 1- Laptop Intel(R) Core (TM) i7-4500U CPU @ 1.80 GHz, 2.40 GHz
- 2- ArcGIS 10.2 software.
- 3- QGIS
- 4- GPSMAP60s Navigator.

2-3- Research flowchart:

Figure (4) reveals the flowchart which was adopted for conducting this research, showing the main steps.

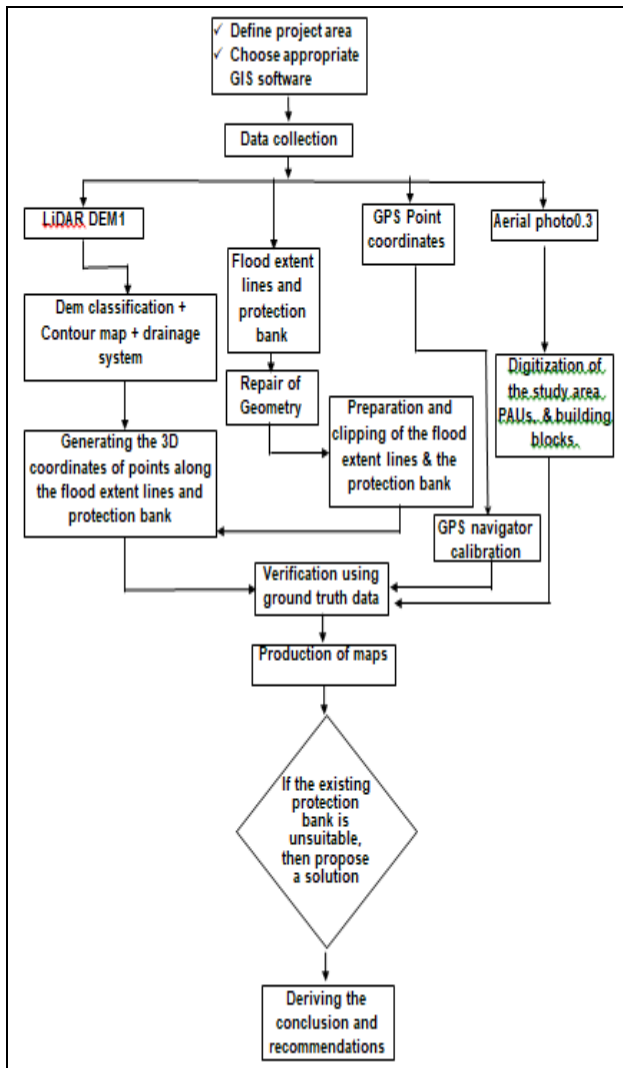


Figure (4): Research flow chart

2-4- Research method description:

Following are the details of the method adopted for carrying out the practical part of the research.

2-4-1- The LiDAR DEM was categorized into 6 classes using the menu item: *Layer properties > Symbology > Classify > then choosing a suitable color ramp*. Result is shown in figure (5). The purpose of the DEM classification is to acquire a clear picture of the relief of the study area. To acquire an even clearer picture of the relief of the study area, a contour map of the study area was produced from the LiDAR DEM using the tool: *Geostatistical Analyst toolbar> Geostatistical Wizard*. Then from the properties of the produced surface, the menu item *Symbology > Classify* was used to fix the contour interval using the equal interval method. The interpolation method used for generating the contour map was the *Inverse Distance Weighted (IDW)*.



2-4-2- Using *ArcHydro tools* to process the LiDAR DEM, the drainage system of the study area was produced. Briefly, the following *ArcHydro* menu items were

used in sequence: 1) *Fill sinks*, 2) *Flow direction*, 3) *Flow accumulation*, 4) *Stream definition*, 5) *Stream segmentation*, 6) *Catchment grid delineation*, 7) *Catchment polygon processing*, 8) *Drainage lines*, 9) *Drainage points*, and 10) *Adjoint catchment processing*.

2-4-3- The blocks of the study area were digitized by the researcher using the 2018 image as a background for editing the blocks, using the *Editor* toolbar. The blocks were overlaid on the PAUs and shown in figure (6).

2-4-4- The flood extent lines of 1946, 1989, and the existing protection bank shapefile obtained from the Surveying Department of Khartoum Locality were processed as follows:

1) Because the original shapefile obtained from the Surveying Department of Khartoum Locality was topologically incorrect, a separate shapefile was produced for the 1946 flood extent line in the following manner:


- a. A new shapefile was created using *ArcCatalogue*, named 1946 flood line.
- b. The *Start Editing mode* of this new shapefile was enabled.
- c. 1946 flood line feature was selected from the original shapefile using the tool: *Select Features*  from the *Editor toolbar*.
- d. The selected 1946 flood line was copied using the tool: *Edit Tool*  from the *Editor toolbar*.
- e. The copied 1946 flood line was pasted in the new shapefile.
- f. The 1946 flood line shapefile was saved.

2) The steps from (a) to (f) were repeated to produce the other two lines, namely the 1989 flood extent line and the protection bank.

2-4-5- Merging the segments of each line:


Each of the lines was found containing more than one segment. Thus, each of them was merged using the menu item: *Merge* contained in the *Editor Menu bar*.

2-4-6- Because the From-nodes and To-nodes of the original lines were not properly organized, it was found necessary to create new continuous lines by tracing each of the lines merged using the tool: *Editor > Trace*. It was decided to divide each of the lines into equal segments (intervals) each interval is 60 m long. Unfortunately, it was found that this process could not be completed using the tool: *Split* contained in the *Editor Menu bar* of ArcGIS10.2. Therefore, the menu item: *Vector > Qchainage* or the

menu item  of the QGIS Desktop 3.4.3.(Madeira) was used to divide each line into 60 m long segments starting from station 0 (at the north) to the end of each line (at the south).

2-4-7- The vertices of each of the lines split were converted into points using the tool: *Arctoolbox> Data*

Management Tool > Features > Feature Vertices To Points.

- 2-4-8- In order to limit the points to the boundary of the study area, the point shapefile was clipped by the study area boundary using the tool: *Analysis Tools > Extract > Clip*.
- 2-4-9- The X,Y coordinates of the points of each of the two flood lines and protection bank were calculated using the tool: *ArcToolbox > Data Management Tools> Features> Add XY Coordinates*.
- 2-4-10- The elevations (Z) of the points of each of 1946, 1989 flood lines and protection bank were calculated from the LiDAR DEM using the tool: *ArcToolbox > 3D Analyst> Functional Surface > Add Surface Information* and the LiDAR DEM as the surface from which the elevation information were acquired.
- 2-4-11- The table containing the population data of the PAUs, obtained from Jabal Awliya locality, was used to calculate the population density of each of the PAUs (Persons/Km²) by dividing the population over the area (in Km²). The calculated density is shown figure (8). The density calculation result of the PAUs was analyzed in conjunction with the 1946 flood extent line.
- 2-4-12- For the analysis of the flood impact on the different PAUs, the flood extent line of 1946 was overlaid on the map of the PAUs' population density.
- 2-4-13- To make sure of the status of the services regarding the flood impact (affected, threatened, or safe), the elevations of the locations of the services should be extracted (calculated) from the LiDAR DEM and compared to the elevations of the corresponding points along the 1946 flood line + 0.30 m (extra height). A problem was faced with ArcGIS 10.2 software when trying to calculate such elevations, hence the Desktop QGIS 3.4.3. tool: *Point Sampling*  was used. Tables (4), (5), and (6) show the affected services, the threatened ones, and the safe ones in the study area. Figure (9) shows the spatial distribution of the same in the study area.
- 2-4-14- The profile of each of the lines (1946, 1989 flood lines and protection bank) were produced from tables A1"obtained from the LiDAR DEM" using Excel menu item: *Insert> Line Graph*.
- 2-4-15- Since the flood level during 1946 was the highest, it was taken as a reference for calculating the necessary height increments to be added to the level of each station of the existing protection bank. The method of calculation and construction of the increments was as follows: Level of flood in 1946 at each station **less** level of the existing protection bank at the nearest station **plus** 0.30 m (extra increment to the level of flood in 1946 in order to safeguard against any future flood level which may exceed that of 1946). For construction purposes, the top surface of the protection bank increments

should have the required slope from chainage station to the next, e.g. as shown in the sketch in figure (5).

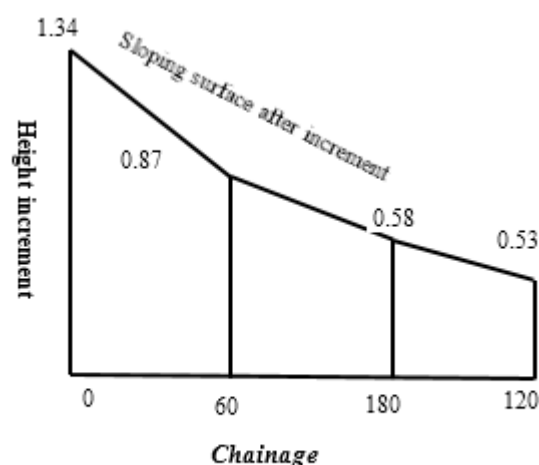


Figure (5): Method of construction of existing protection bank increments

Table (1): Sample of increments extracted from table (A2)

| Chainage | Flood 46 level | Protection level | 46 flood - protection | 46-protection + 0.3 m |
|----------|----------------|------------------|-----------------------|-----------------------|
| 0 | 383.70 | 382.66 | 1.04 | 1.34 |
| 60 | 383.86 | 383.28 | 0.57 | 0.87 |
| 120 | 384.15 | 383.87 | 0.28 | 0.58 |
| 180 | 384.27 | 384.03 | 0.23 | 0.53 |

2-4-16- Ground truth using Garmin GPSMAP60CSx navigator:

On Sept. 02, 2021 AD., the PhD. student carried out a field work aiming at collecting points coordinates to be used for ground truthing and to get a general idea about the topography of the study area "Azozab".

To get the altitudes at the ground surface, the measured altitudes were reduced by 0.65 m which the height above the ground surface at which the navigator was held.

3- Results and Discussions:

4-1- Classified LiDAR DEM 1m and contour map:

In order to get a clear picture of the topography of the study area, the LiDAR DEM was classified and a contour map was produced from it and shown in figure (6). The contour interval (height variation) was 0.5 m. As expected, the area adjacent to the White Nile is the lowest area (the elevations range from 375.91 m to 382 m above mean sea level). The highest area is located at the south-eastern part and most of the western part of the study area, (the elevations range from 383.25 m to 388.54 m above mean sea level). The elevations of the rest of the study area are medium (elevations range from 382.01 m to

383.24 m above mean sea level). Refer to the legend of the classified LiDAR DEM in figure (6).

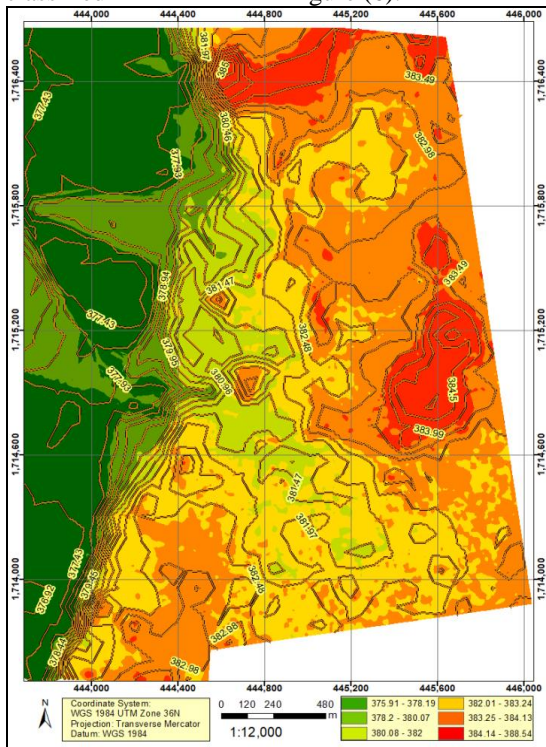


Figure (6): Classification of the LiDAR Dem and Contours

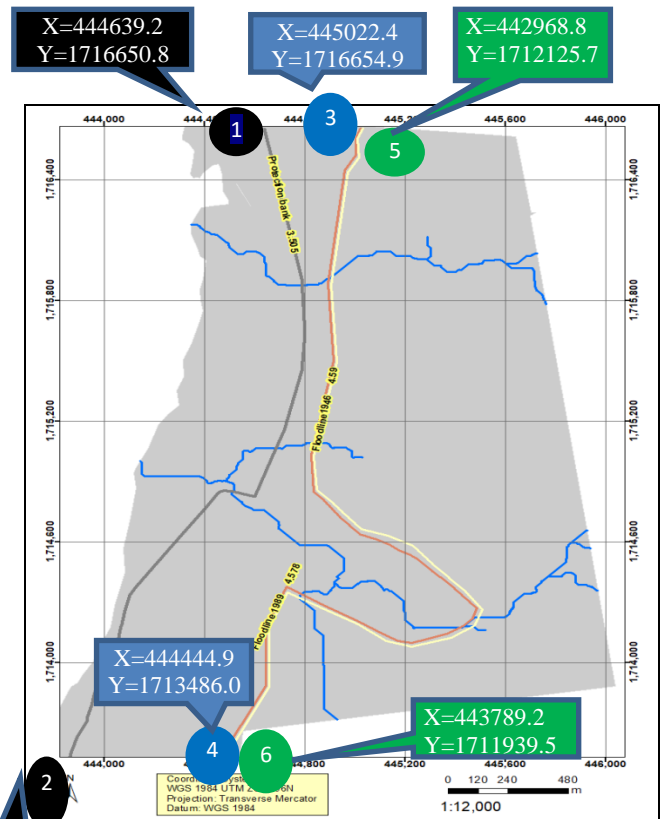


Figure (7): Flood lines and protection bank after clipping using Azozab area

4-2- Flood extent (1946 & 1989) and protection bank:

The polylines shapfiles (showing flood extent in 1946, 1989 & the existing protection bank) after they have geometrically corrected and before and after clipping using the study area boundary are shown in figures (7) respectively. The planimetric coordinates of the start and end of each of the flood extent lines and the protection bank after being clipped using the boundary of the study area are shown in table (2).

Table (2): Coordinates of the start and end points

| Point No. | Line name | X-start | Y-start | X-end | Y-end |
|-----------|------------------------|-----------|-------------|-----------|-------------|
| 1 | Flood extent line 1946 | 445,031.7 | 1,716,654.1 | | |
| 2 | | | | 444,473.5 | 1,713,511.5 |
| 3 | Flood extent line 1989 | 445,022.9 | 1,716,656.2 | | |
| 4 | | | | 444,451.7 | 1,713,499.6 |
| 5 | Protection line | 444,639.2 | 1,716,650.8 | | |
| 6 | | | | 443,865.3 | 1,713,533.3 |

4-3- Population density Analysis:

From table (3), which shows the population density in the study area, it is clear that the highest population density is at Wad Ajeeb unit (16,518 persons/Km²) followed by Kalakla Gala Blk 2 (15,488 persons/Km²), then ELazozab BLK 2-3 (13,360 persons/Km²), and Al Dabasin West (13,091 persons/Km²) which are listed at the top of table (4-2) while the lowest density is at Alfarog blk1 (4,344 persons/Km²) which is listed under serial number (11) in the table.

Table (3): Population density in the study area

| PAU_Name | Population | Area (m ²) | Area (Km ²) | Density (Persons/Km ²) |
|--------------------|------------|------------------------|-------------------------|------------------------------------|
| Wad Ajeeb | 3,368 | 203,904.8 | 0.2039048 | 16,518 |
| Kalakla Gala BLK 2 | 5,066 | 327,084 | 0.3270824 | 15,488 |
| ELazozab BLK 2-3 | 9,007 | 598,498 | 0.5984928 | 13,360 |
| Al Dabasin West | 2,337 | 178,513 | 0.1785173 | 13,091 |

| | | | | |
|---------------------------|--------------|-----------------------|-----------------------|--------------|
| Yathrib | 3,221 | 297,25 2.4 | 0.297252 4 | 10,836 |
| Alazozab BLK 1 | 2,376 | 230,10 4.1 | 0.230104 1 | 10,326 |
| Alray Almasri | 3,604 | 354,04 0.1 | 0.354040 1 | 10,182 |
| Al Dabasin East | 2,957 | 301,86 5.3 | 0.301865 3 | 9,796 |
| Kalakla Gala BLK 1 | 3,265 | 381,86 3.3 | 0.381863 3 | 8,550 |
| Al Farog BLK 3-10 | 4,175 | 688,45 3.1 | 0.688453 1 | 6,064 |
| <i>Al Farog BLK 1</i> | <i>1,268</i> | <i>291,90 1.5</i> | <i>0.291901 5</i> | <i>4,344</i> |

Furthermore, from figure (8), which shows the highest flood line (46) overlaid on the PAUs' population density map, the four high density population PAUs, which are listed at the top of table (3), should be given more attention in order to avoid destructive flood risks.

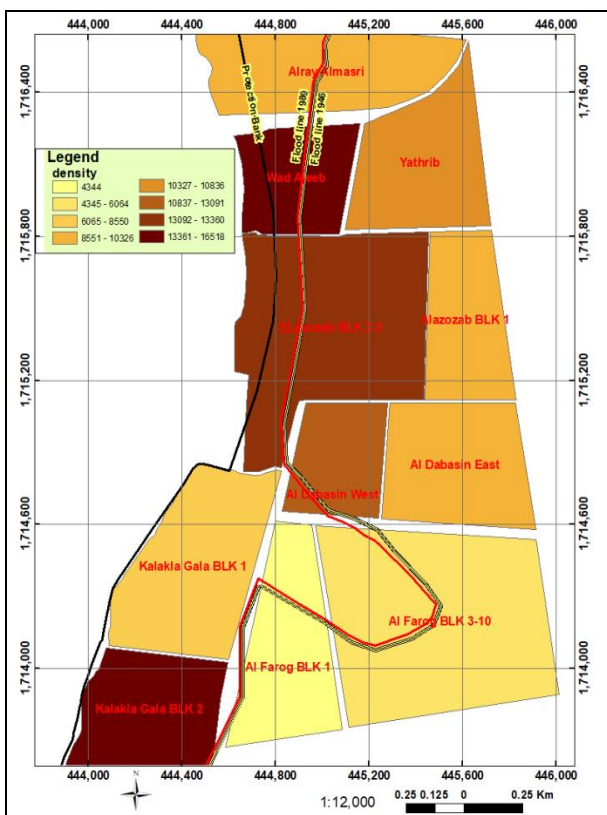


Figure (8): Population Density in the study area

4-4- The situation of services in the study area:

Analysis result of the situation of the services - with respect to the flood impact -existing in the study area is shown in tables

(3) affected services, (4) threatened services, and (5) safe services, as well as figure (9).

1. Affected services:

These are service located inside the flood extent of 1946 and they include 5 mosques +3 Education + 1 health + 1 WP + 1 PS = 11

Table (4): Affected services

| SN | Service type | Elevation (m) | Elevation rank |
|-----------|---------------|---------------|----------------|
| 1 | PS | 381.80 | |
| 2 | Mosque | 381.77 | |
| 3 | Education | 381.40 | |
| 4 | Mosque | 382.36 | |
| 5 | Health | 382.45 | |
| 6 | WP | 382.34 | |
| 7 | Education | 382.50 | |
| 8 | Education | 382.56 | |
| 9 | Mosque | 381.77 | |
| 10 | Mosque | 382.65 | Max. |
| 11 | Mosque | 380.94 | Min. |

II. THREATENED SERVICES

These are the services located at Threatened services are 8 educational ones.

Table (5): Threatened services

| SN | Service type | Elevation (m) | Elevation rank |
|-----------|------------------|---------------|----------------|
| 1 | Mosque | 382.54 | |
| 2 | Mosque | 382.64 | |
| 3 | Education | 385.04 | Max. |
| 4 | Mosque | 384.79 | |
| 5 | Mosque | 382.78 | |
| 6 | Mosque | 383.08 | |
| 7 | Church | 383.23 | |
| 8 | Mosque | 382.70 | |
| 9 | Mosque | 382.94 | |
| 10 | Health | 382.38 | |
| 11 | Education | 382.65 | |
| 12 | Education | 382.40 | |
| 13 | WP | 382.88 | |
| 14 | Market | 382.52 | |
| 15 | Health | 382.28 | Min. |
| 16 | Education | 382.66 | |
| 17 | Education | 383.08 | |
| 18 | Mosque | 382.88 | |
| 19 | Education | 382.55 | |

2. Safe services:

| SN | Service type | Elevation (m) | Elevation rank |
|----|------------------|---------------|----------------|
| 1 | Mosque | 382.54 | |
| 2 | Mosque | 382.64 | |
| 3 | Education | 385.04 | Max. |
| 4 | Mosque | 384.79 | |
| 5 | Mosque | 382.78 | |
| 6 | Mosque | 383.08 | |
| 7 | Church | 383.23 | |
| 8 | Mosque | 382.70 | |
| 9 | Mosque | 382.94 | |
| 10 | Health | 382.38 | |
| 11 | Education | 382.65 | |
| 12 | Education | 382.40 | |
| 13 | WP | 382.88 | |
| 14 | Market | 382.52 | |
| 15 | Health | 382.28 | Min. |
| 16 | Education | 382.66 | |
| 17 | Education | 383.08 | |
| 18 | Mosque | 382.88 | |
| 19 | Education | 382.55 | |

Safe services include 8 mosques + 6 education + 2 health + 1 Market + 1 church + 1 WP.

Table (6): Threatened services

The total number of services in the study area is 38 ones, according the following details: 19 safe services + 8 threatened ones +11 affected ones

Affected services are the ones which are located inside the flood extent of 1946 and shown in the map in a red-coloured symbol and label, threatened ones are those located within 200 meters away from the flood extent line of 1946 and shown in the map in a black-coloured symbol and label, and safe ones are those located at a distance that exceeds 200 meters from the flood extent line of 1946 and shown in the map in a green-coloured symbol and label.

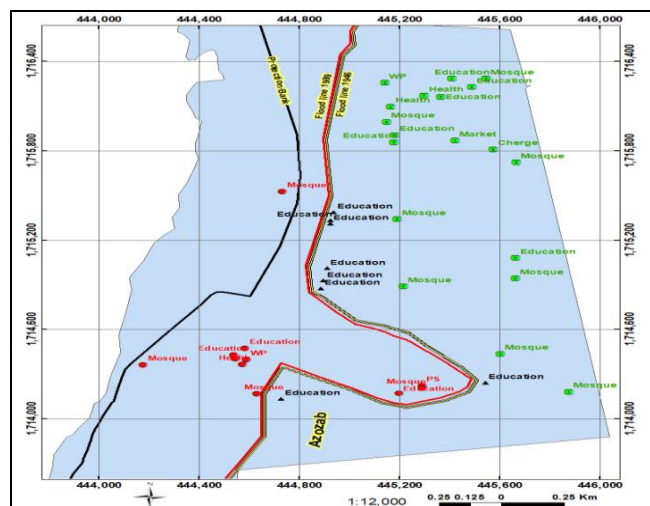


Figure (9): Flood affected services in the study area

4-5- Three Dimensional Coordinates of the 3 lines from LiDAR DEM:

| SN | Statistic | Value | | |
|----|-------------------------|-------------|------------|-------------|
| | | Flood 46 | Flood 89 | Protection |
| 1- | Count | 77 | 77 | 59 |
| 2- | Total of elevations | 29,444.92 | 29,439.93 | 22,509.81 |
| 3- | Max. elevation | 384.27 | 384.20 | 384.97 |
| 4- | Min. elevation | 380.83 | 380.60 | 379.43 |
| 5- | Variation (Max. – Min.) | 3.44 | 3.60 | 5.54 |
| 6- | Mean | 382.40 | 382.34 | 381.52 |
| 7- | Sum of diff^2 | 40.43864867 | 46.1541965 | 76.17878 |
| 8- | (Sum of diff^2)/N | 0.525177 | 0.59940514 | 1.291131867 |
| 9- | Standard deviation | 0.724691 | 0.774206 | 1.136279837 |

Table (A4) in the appendices shows the X,Y coordinates of points (at 60 m planimetric interval) and the elevations (Z) of the same points along each of the flood 46, flood 89, and protection lines extracted from LiDAR DEM. The statistical analysis of the elevations of the three lines yielded the statistics included in table (7).

Table (7): The statistics of the 3 lines' elevations from LiDAR DEM

Figure (10) shows the profile “the elevations (Z) plots” of the points along each of the flood 46, flood 89, and protection line extracted from the LiDAR DEM.

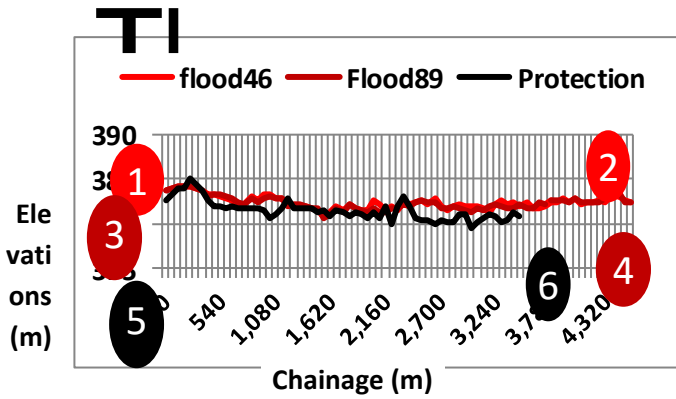


Figure (10): Elevations of points along the 3 lines from LiDAR DEM

4-6- Protection bank height increasing:

5- Table (A9) in the appendices and figure (11) show the increments which are to be added to the protection line heights in order to be equal to the level of the flood line in 1946. In addition to the difference shown in the figure, an extra height of 0.30 m should be added at each station to provide for any future flood level that may exceed the level of 1946 flood.

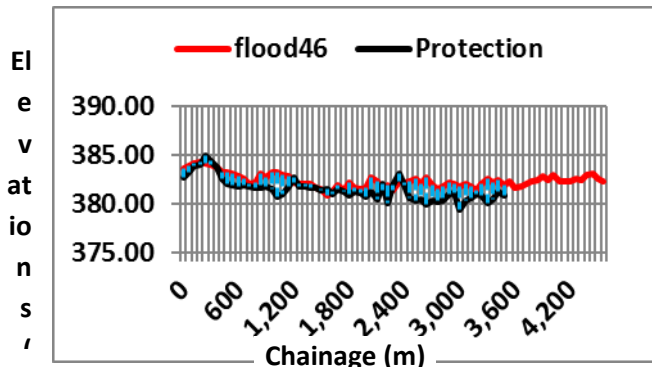


Figure (11): Protection bank height increments (reference is 1946 flood line)

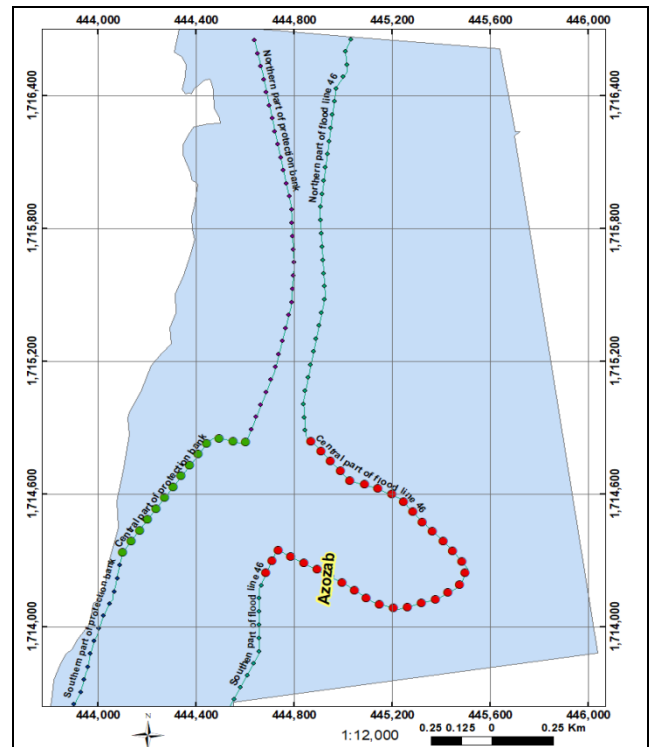


Figure (12): Increasing the protection bank height

5-1- Ground truth:

Table (8) shows the statistics of the altitudes captured in the field. The statistics of 71 points coordinates captured at the field using GPS navigator .

Table (8): Statistics of the altitudes captured in the field

| SN | Statistic | Value |
|----|--------------------|-----------|
| 1- | Count | 71 |
| 2- | Sum | 27,482.14 |
| 3- | Max. | 387.82 |
| 4- | Min. | 385.72 |
| 5- | Variation | 2.10 |
| 6- | Mean | 387.07239 |
| 7- | Sum of diff^2 | 32.67631 |
| 8- | (Sum of diff^2)/N | 0.4232013 |
| 9- | Standard deviation | 0.650539 |

From table (8), it is found that the standard deviation is 0.650539, a value which suggests that the field-collected elevations were precise and fairly clustered around the mean.

III. CONCLUSION AND RECOMMENDATIONS

4-1- Conclusion:

Flood is the deadliest type of severe weather. The use of remotely sensed data and Geographic Information Systems (GIS) in flood monitoring and management proved to be very helpful. The study area “Azozab” locality, Khartoum state, Sudan used to be exposed to severe floods frequently, mainly because of the White Nile floods accompanied by storm waters during the rainy season. In view of this fact, the study aims to contribute to the effort for mitigating the adverse impact of floods in the study area, via the analysis of the most severe floods (in 1946 and 1989) as well as the effectiveness of the existing protection bank built along the White Nile’s bank adjacent to the study area.

The 2D (planimetric) coordinates (X, Y) of points along each of the flood extent lines 1946, 1989, and the existing protection bank were obtained from the shapfile of each line, while the elevations (Z-coordinates) of the same points were obtained from the digital elevation model of the study area. Light Detection And Ranging DEM1m was used. LiDAR elevations (fishnet) points yielded a mean of 383.118 and a standard deviation of 0.749.

The point coordinates of the mentioned lines (obtained from LiDAR DEM) were plotted as graphs. By Comparison of the lengths of the 3 lines, it was found that the flood line 1946 is 4.59 km long, flood line 1989 is 4.57 km long, and the protection bank is 3.5 km long, therefore, the protection bank should be extended so that its length becomes equal to the length of 1946 flood line, i.e. to be extended by 1.09 Km, while comparison of the elevations of the points along the 3 lines reveals that Moreover, the elevations of the protection bank were found lower than the elevations of both flood lines for a distance of 3.02 km i.e. a percentage of 86.1% of its total length which represents the length of the protection bank that requires increasing its elevations (i.e.to construct a higher embankment).

4-2- Recommendations:

The authrs have recommended the following:

1. The height of the protection bank should be raised by 1.2 m (in average) in order to guard against any future high floods. The height of the highest past flood level (i.e. the flood of 1946) should be taken as a reference, but extra 30 cm should be added to the height of 1946 flood line chainage stations as necessary to safeguard against the flood risk if the height of a future flood exceeds that of 1946.
2. If the digital elevation model (to be used) contains artifacts, they should be removed, and the accuracy of the digital elevation model should be verified.
3. The spatial reference of all of the used datasets should be unified.
4. The use of remotely sensed datasets is recommended for similar studies (particularly, if the study requires repeated data acquisition), because remote sensing facilitates the acquisition of information from a wide area, but the use of such data should be accompanied by field work for the acquisition of ground truth data.
5. Also, the geographic information system techniques should be exploited, since these techniques enables the analysis of spatial data in an efficient manner.
6. If sufficient flood and rainfall monitoring data is available for many years, this will support building a rich and comprehensive database, which, in turns, supports building a reasonable model for predicting flood extent, and consequently support making a suitable decision in this concern.
7. Some other methods for mitigation of the floods impact can be further studied such as the implementation of rainwater harvesting projects at locations across the water courses (valleys) existing within and outside the study area. Consequently, the quantity of the storm water heading to the White Nile through such valleys is minimized, a situation which leads to the mitigation of the White Nile floods. Likewise, construction of dams at suitable sites across the White Nile can be useful to mitigate the impact of the White Nile floods.

REFERENCES

- Adda, P., Mioc, D., Anton F., McGillivray E., Morton A. & Fraser, D. (2013). 3d flood-risk models of government infrastructure, https://isprs.org/proceedings/xxxviii/4-w13/id_39.pdf.
- Altayeb H. Yahya, Low-cost space-related technologies for flood mitigation and monitoring, Case study: Sharg Elneel locality, Khartoum State, Sudan. Paper presented at the International University of Africa Disaster Management and refugees Studies Institute (DIMARSI) workshop under the title “Role of the base societies in limiting the disaster risks “Tuti as a sample”. In the period 19-20/04/2014.
- Altayeb H. Yahya, Volume of water to be harvested using space Technologies Case study: Part of Khartoum State in Sudan presented at ISNET / RJGC Workshop on Applications of Satellite Technology in Water Resources Management, 18 - 22 Sep 2011; Amman, Jordan.
- Bater, C.W. & Coops, N.C (2009). Evaluating error associated with lidar-derived DEM interpolation. *Computers & Geosciences* 35: pp. 289-300.
- Bodoque, J.M., Guardiola-Albert, C., Aroca-Jiménez, E., Eguibar, M.A. & Martínez-Chenoll, M.L. (2016). Flood Damage Analysis: First Floor Elevation Uncertainty Resulting from LiDAR-Derived Digital Surface Models, <https://doi.org/10.3390/rs8070604>.
- Bodoque, J.M., Guardiola-Albert, C., Aroca-Jimenez, E., Angel Eguibar, M. & Martinez-Chenoll, M.L. (2016). Flood damage analysis: first floor elevation uncertainty resulting from LiDAR-derived digital surface models, *Remote Sens* 8: pp. 604, <https://doi.org/10.3390/rs8070604>.
- Brzank, A., Heipke, C., Goepfert, J. & Soergel, U. (2008). Aspects of generating precise digital terrain models in Wadde Sea from lidar—water classification and structure line extraction. *ISPRS J Photogramm Remote Sens* 63: pp. 510–528. <https://doi.org/10.1016/j.isprsjprs.2008.02.002>.

- Dowding, S., Kuuskivi, T. & Li, X. (2004). Void fill of SRTM Elevation Data —Principles, Processes and Performance. Proceedings of the Conference “ASPRS Images to Decision: Remote Sensing Foundation for GIS Applications”, Kansas City, MO.
- Evans, Y. S., Gunn, N. & Williams, D., (2008). Use of GIS in Flood Risk Mapping, CorpusID:14652610,<http://idrcgisworkshop.pbworks.com/f/Use+of+GIS+in+flood+risk+Mapping.pdf>
- Foni, A. & Seal, D. (2004). Shuttle Radar Topography Mission: An Innovative Approach to Shuttle Orbital Control. *Acta Astronautica*, 54, pp. 565–570.
- Gebrehiwot, (2018). Challenges and Opportunities for UAV-Based Digital Elevation Model Generation for Flood-Risk Management: A Case of Princeville. <https://doi.org/10.3390/s18113843>, Corpus ID: 53306101
- Gizachew, K., (2017). LiDAR DEM Data for Flood Mapping and Assessment; Opportunities and Challenges, <https://doi.org/10.4172/2469-4134.1000211>
- Hailea, A.T. & Rientjesb, T.H.M. (2004). Effects of LIDAR DEM resolution in flood modelling: A model sensitivity study for the city of Tegucigalpa, Honduras, <https://isprs.org/proceedings/xxxvi/3-w19/papers/168.pdf>
- Hashemi-Beni, L., Jones, J., Thompson, G., Johnson, C., McDougall K. & Temple-Watts P., (2012). The use of lidar and volunteered geographic information to map flood extents and inundation, Vol. I-4, XXII ISPRS Congress, Melbourne, Australia
- Hatzopoulos, J. N. (2002). Geographic Information Systems (GIS) in water management, <https://doi.org/10.1007/BF00508896>
- Hawker, L., Bates, P., Neal, J. & Rougier, J. (2018). Perspectives on Digital Elevation Model (DEM) Simulation for Flood Modeling in the Absence of a High-Accuracy Open Access Global DEM, Vol. 6, Article 233, <https://doi.org/10.3389/feart.2018.00233>
- Hoefle, B., Vetter, M., Pfeifer, N., Mandlbürger, G. & Stotter, J. (2009). Water surface mapping from airborne laser scanning using signal intensity and elevation data. *Earth Surf Process Landforms* 34(12): pp. 1635–1649. <https://www.geodose.com/2019/03/spatial-interpolation-inverse-distance-weighting-idw.html>
- Islam, M. (2000). Flood damage and management modeling using satellite remote sensing data with GIS: case study of Bangladesh, ISBN: 1901502465, Corpus ID: 127105631 pp. 455-457 ref.2.
- J. R. Ternate, M. I. Celeste, E. F. Pineda, F. J. Tan, and F. A. A. Uy. (2017). Floodplain Modelling of Malaking-Ilog River in Southern Luzon, Philippines Using LiDAR Digital Elevation Model for the Design of Water-Related Structures, <https://doi.org/10.1088/1757-899X/216/1/012044>
- Jakovljevic, G. & Govedarica, M. (2018). Water Body Extraction and Flood Risk Assessment Using Lidar and Open Data, https://doi.org/10.1007/978-3-030-03383-5_7
- Jared P. ENO., Anne M. Linn, (2016). Flood Progression Modeling and Impact Analysis.
- Jarvis, A., Rubiano, J., Nelson, A., Farrow, A. & Mulligan, M. (2004). Practical use of SRTM data in the tropics—comparisons with digital elevation models generated from cartographic data. Working Document, Vol. 198. Centro Internacional de Agricultura Tropical (CIAT), pp. 32.
- Kaab, A. (2005). Combination of SRTM3 and repeat ASTER data for deriving alpine glacier flow velocities in the Bhutan Himalaya. *Remote Sensing of Environment*, 94, pp. 463–474.
- Kaplan, G. & Avdan, U. (2017). Object-based water body extraction model using Sentinel-2 satellite imagery. *Eur J Remote Sens* 50(1): pp. 137–143, <https://doi.org/10.1080/22797254.2017.1297540>
- Kellndorfer, J., Walker, W., Pierce, L., Dobson, C. & Fites, J.A. (2004). Vegetation height estimation from Shuttle Radar Topography Mission and National Elevation Datasets. *Remote Sensing of Environment*, 93, pp. 339–358, <https://doi:10.1016/j.rse.2004.07.017>.
- Koch, A. & Lohmann, P. (2000). Quality Assessment and Validation of Digital Surface Models derived from the Shuttle Radar Topography Mission (SRTM), IAPRS, Vol. XXXIII, Amsterdam, pp. 3.
- Mehebab, S., Sajjad, H. & Ahmed, R. (2015). Assessing flood inundation extent and landscape vulnerability to flood using geospatial technology: A study of Malda district of West Bengal, India, Vol. XIV, pp. 156-163, <http://dx.doi.org/10.5775/fg.2067-4635.2015.144.d>
- Miliareisis, G.C. & Paraschou, C.V.E. (2005). Vertical Accuracy of SRTM DTED Level 1 of Crete. *International Journal of Applied Earth Observation and Geoinformation*, 7, pp. 49-59.
- National Research Council of the National Academies (2009) Mapping the zone, improving flood map accuracy. The National Academies Press, Washington, DC., ISBN 978-0-309-13057-8, pp. 7, <https://doi.org/10.17226/12573>.
- Ouma Y., Tateishi R., 2014, Urban Flood Vulnerability and Risk Mapping Using Integrated Multi-Parametric AHP and GIS: Methodological Overview and Case Study Assessment., pp. 1515-1545, <https://doi.org/10.3390/w6061515>.

- Ozah, A.P. and Kufoniyi, O. (2008). Accuracy assessment of Contour Interpolation from 1:50,000 Topographical maps and SRTM data for 1:25,000 Topographical Mapping. The International Archives of the Photogrammetry, Remote Sensing and Spatial Information Sciences. Vol. XXXVII. Part B7. sharpening. Remote Sens9(6): pp. 596, <https://doi.org/10.3390/rs9060596>.
- Rabus, B., Eineder, M., Roth, A. & Bamler, R. (2003). The Shuttle Radar Topography Mission – a new class of Digital Elevation Models acquired by spaceborne Radar. ISPRS Journal of Photogrammetry and Remote Sensing, 57, pp. 241–262.
- Smeckaert, J., Mallet, C., David, N., Chehata, N. & Ferraz, A. (2013). Large-scale water classification of coastal areas using airborne topographic LiDAR data. In: IEEE International Geoscience and Remote Sensing Symposium, Melbourne, VIC, Australia, <https://doi.org/10.1109/igarss.2013.6721092>.
- Smith, J. & Rowland, J., (2006). Temporal Analysis of Floodwater Volumes in New Orleans After Hurricane Katrina, <https://doi.org/10.3133/cir13063H>.
- Topaloglu, R. H, Sertel, E. & Musaoglu, N. (2016). Assessment of classification accuracies of Sentinel-2 and Landsat-8 data for land cover/use mapping. In: The International Archives of the Photogrammetry, Remote Sensing and Spatial Information Sciences, Vol XLI-B8, XXIII ISPRS Congress, 12–19 July 2016, Prague, Czech Republic. <https://doi.org/10.5194/isprsarchives-xli-b8-1055-2016>.
- University of Southern Queensland (2015). DEM Generation and Hydrologic Modelling using LiDAR Data, vol. 1, Student number: 0050102572, pp. 26-27.
- Van de Sande, B., Lansens, J. & Hoyng, C. (2012). Sensitivity of coastal flood risk assessments to digital elevation models. Water, Vol. 4, pp. 568–579. <https://doi.org/10.3390/w4030568>.
- Van Zyl, J.J. (2001). The Shuttle Radar Topography Mission (SRTM): A breakthrough in remote sensing of topography. Acta Astronautica, 48(5–12), pp. 559–565.
- Verpoorter, C., Kutser, T. & Tranvik, L. (2012). Automated mapping of water bodies using Landsat multispectral data. Limnol Oceanogr Methods 10:1037–1050. <https://doi.org/10.4319/lom.201210.103>
- Wedajo, G.K. (2017). LiDAR DEM data for flood mapping and assessment; opportunities and challenges - a review. J Remote Sens GIS 6:4. <https://doi.org/10.4172/2469-4134.1000211>.
- Yang, X., Zhao, S., Qin, X., Thao, N. & Liang, L. (2017). Mapping of urban surface water bodies from Sentinel-2 MSI imagery at 10 m resolution via NDWI-based image